Pseudo Peak Suppression in Generating Range Profile with Multi-carrier Chirp

YANG Chao[1], ZHENG Lin[1,2], BAI Yunhao[1]
1. Key Lab. of Cognitive Radio & Information Processing, the Ministry of Education, Guilin, P. R. China
2. Sci. and Tech. on Info. Transmission and Dissemination in Communication Networks Laboratory, Shijiazhuang, P. R. China
1124574616@qq.com, gwzheng@gmail.com

Abstract: - To ensure the reliability of transmission and prevent inter-carrier interference (ICI) between sub-bands, the sub-carrier frequency increment is usually greater than the bandwidth of sub-band for multi-carrier chirp. That will bring on false targets generated by pseudo peaks on High Resolution Range Profile (HRRP). At the presence of false targets, it is difficult to get the true position of target due to the serious influence on target detection. In this paper, the mechanism of pseudo peaks generation is analyzed and an algorithm is proposed to remove pseudo peaks while the image resolution is improved by Super-SVA, which reduces the echo pulse width. With the pulse width less than an unambiguous range, the HRRP without false targets can be obtained. With the analysis and simulation of single and multi-targets, the results indicate that this algorithm can effectively remove false targets caused by the pseudo peaks.

Key-Words: - Multi-carrier communications; pseudo peak; Super-SVA; HRRP, Target detection, Chirp signal

1 Introduction

The combination with communication and target detection is an important application area on Radar-communication integration. In communication areas, it is based on wireless network to achieve collaborative target perception. Multi-carrier signal can improve the information transmission rate as a communication signal, and is also able to synthesize large bandwidth to obtain HRRP as a radar signal. Therefore, multi-carrier chirp signal becomes more important in the research area of radar communication integration[1~3].

Compared with multi-carrier chirp, stepped-frequency chirp signal (SFCS) is widely used in modern high-resolution radar, which has a low hardware complexity since it uses a narrowband transceiver. However, without parallel transmission in subbands, SFCS has a lower information transmission rate than that of multi-carrier chirp. Meanwhile, due to Doppler affection, SFCS generates linear phase item and quadratic phase term which results in target range shift and echo spread[4]. Multi-carrier chirp signal has the characteristics of being insensitive to Doppler, that is, it is immune to Doppler influence in moving targets[5].

To obtain HRRP with multi-carrier chirp, first step in digital processing is channel division for different sub-band. After pulse compression, each sub-chirp signal becomes a coarse resolution range profile (called coarse distance dimension). Then, HRRP is obtained via IDFT applied to different channels in the same coarse range gate, which is called as fine distance dimension. To reduce the loss of oversampling, higher sampling frequency than the bandwidth of sub-band must be adopted, which result in over-sampling result of pulse compression. So the target pick-up algorithm has to be adopted to eliminate target's redundancy in order to obtain fine HRRP. In target extraction[6,7], a zone is picked up from each fine distance dimension, called valid zone here. And there is only one valid zone for a single target under the ideal condition.

In order to ensure the reliability of transmission and prevent inter-carrier interference (ICI) between sub-bands, it is essential to add a guard interval or use a time-frequency domain roll-off shaping filter between sub-bands for multi-carrier communication signal. As a result, the carrier frequency increment Δf must be greater than bandwidth of subband B, as shown Figure 1. At this point, the pulse width is greater than the unambiguous range in the synthetic range profile. Hence, more than one valid zone occurs in a pulse width. After target extraction, false targets will turn up inevitably in range profile, which impact on the target detection.

This paper analyzes the mechanism of pseudo peaks generation, and proposes the algorithm of pseudo peaks suppression based on the spectrum extrapolation characteristics of Super-SVA. That

makes pulse width less than an unambiguous range by increasing bandwidth of echo signal. The algorithm can avoid the generation of false targets and improve the resolution of the target. The results of computer simulation are given in agreement with the analysis.

2 HRRP synthesizing principle with multi-carrier chirp

The mathematic expression of multi-carrier chirp transmitted signal is given by

$$f\left(t\right)=\frac{1}{\sqrt{N}}\sum_{i=0}^{N-1}u\left(t\right)\cdot\exp\left(j2\pi\left(f_0+i\Delta f\right)t\right) \quad (1)$$

where

$$u\left(t\right)=\frac{1}{\sqrt{T}}rect\left(\frac{t}{T}\right)\exp\left(j\pi kt^2\right)$$

and $u\left(t\right)$ is the baseband signal of the chirp. $k=B/T$ is the frequency-modulation slope of a subband chirp, B is the bandwidth of subband chirp, and T is the symbol width. N and i are the number and the index of carry frequencies respectively. f_0 is the initial carrier frequency, Δf is the carrier frequency increment of subband chirp. The time-frequency diagrams of signal are as shown in Figure 1.

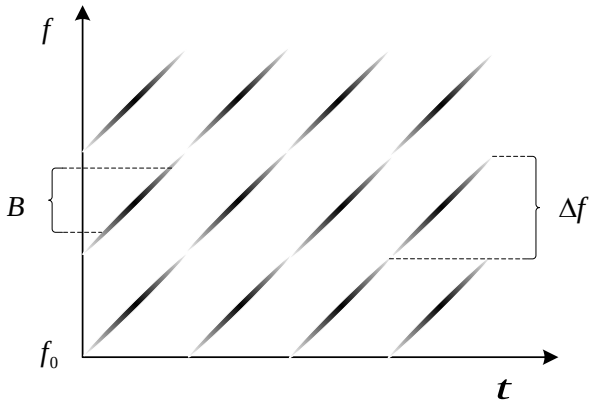

Fig.1: The time-frequency diagrams of signal

The echo signal of multi-carrier chirp is expressed as:

$$f\left(t\right)=\frac{1}{\sqrt{T}}\sum_{i=0}^{N-1}u\left(t-\tau\left(t\right)\right)\cdot\exp\left(j2\pi\left(f_0+i\Delta f\right)\left(t-\tau\left(t\right)\right)\right) \quad (2)$$

where

$$u\left(t\right)=\frac{1}{\sqrt{T}}rect\left(\frac{t}{T}\right)\exp\left(j\pi kt^2\right)$$

Considering the insensitivity to Doppler for multi-carrier chirp, the target is supposed to be a stationary. So the echo delay of target is $\tau\left(t\right)=2R/c$, where R is the range of target and c is the light speed.

After channel division, the baseband signal is given by

$$f_i\left(t\right)=\frac{1}{\sqrt{N}}u\left(t-\tau\left(t\right)\right)\cdot\exp\left(j2\pi\left(f_0+i\Delta f\right)\left(-\tau\left(t\right)\right)\right) \quad (3)$$

Using pulse compression[10] on baseband signal of different channel, Equation (3) becomes

$$S_i\left(t\right)=\sqrt{kT^2}\cdot rect\left[\frac{t-2R/c}{T}\right]\cdot\frac{\sin\pi kT\left(\mathrm{t}-2R/c\right)}{\pi kT\left(t-2R/c\right)}\cdot\exp\left(-\pi k\left(t-2R/c\right)^2\right)\cdot\exp\left(j\pi/4\right)\cdot\exp\left(-j2\pi i\Delta f\cdot 2R/c\right)\cdot\exp\left(-j2\pi f_0\cdot 2R/c\right) \quad (4)$$

Sampling $S_i\left(t\right)$ at $t=2R/c$, and it yields:

$$S_i\left(\frac{2R}{c}\right)=\sqrt{kT^2}\cdot\exp\left(j\pi/4\right)\cdot\exp\left(-j2\pi i\Delta f\cdot 2R/c\right)\cdot\exp\left(-j2\pi f_0\cdot 2R/c\right) \quad (5)$$

Taking N-point IDFT of $S_i\left(2R/c\right)$ with respect to i, we can obtain the HRRP of the target as follows:

$$S_{IDFT}=\sqrt{kT^2}\cdot\left|\frac{\sin\pi\left(l-N\Delta f\cdot 2R/c\right)}{N\sin\pi\left(l/N-\Delta f\cdot 2R/c\right)}\right| \quad (6)$$

3. Mechanism of pseudo-peak generation

Figure 2 is the 2 dimensional range profile under $B=\Delta f$. In the figure, the horizontal axis represents the coarse distance dimension, on which the interval between each slash is sampling range resolution r_s, $r_s=cT_s/2$, where T_s is the sampling interval. The slash axis represents the fine distance dimension, and different slash corresponds to different distance gate, whose length is called the single point unambiguous range r_I. Each rough line

is a valid zone of different distance gate on the fine distance dimension, which is same as r_s in length. When all slashes connect up in order, HRRP can be obtained.

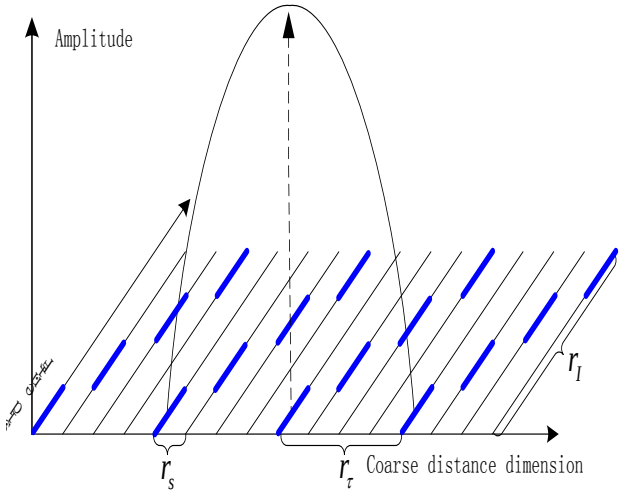

Fig.2: The 2 dimension range profile under $B = \Delta f$

It assumes that $r_\tau = 4r_s$ in Figure 2, where r_τ is the distance resolution of a pulse. As shown in coarse distance dimension, there are only 4 sampling points between the center of mainlobe and first zero point. Meanwhile, the single point distance unambiguous range is equal to 4 times length of a valid zone, that is $r_I = 4r_s$, which locates on different place in each distance gate. In the case, the only one sampling point in a single pulse can fall into the valid zone. so there is only one sampling point to be saved for each target after target extraction.

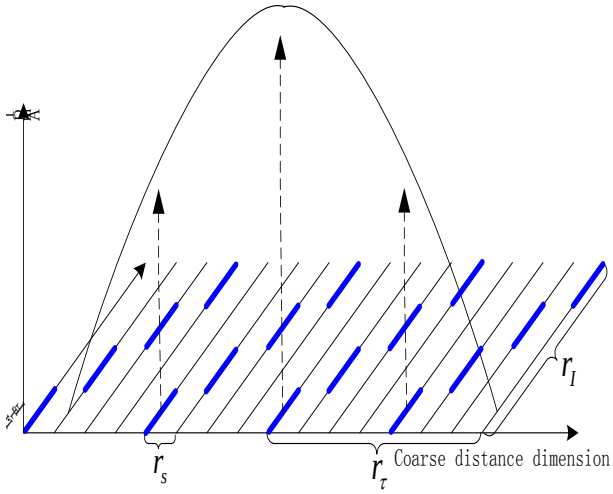

Fig.3: The 2 dimension range profile under $B < \Delta f$

It assumes that $B = f_s/7$, $\Delta f = f_s/4$,when $B < \Delta f$ shown in Figure 3.

In Figure 3, there are 7 sampling points between the center of mainlobe and first zero point in a single pulse, and the single point distance unambiguous range is equal to 4 times length of an valid zone. However, there are 3 sampling points falling into the valid zone in a single pulse. As a result, two false targets will turn up in HRRP, which impact on the target detection.

4. Super-SVA on multi-carriers chirp

3.1 Super-SVA

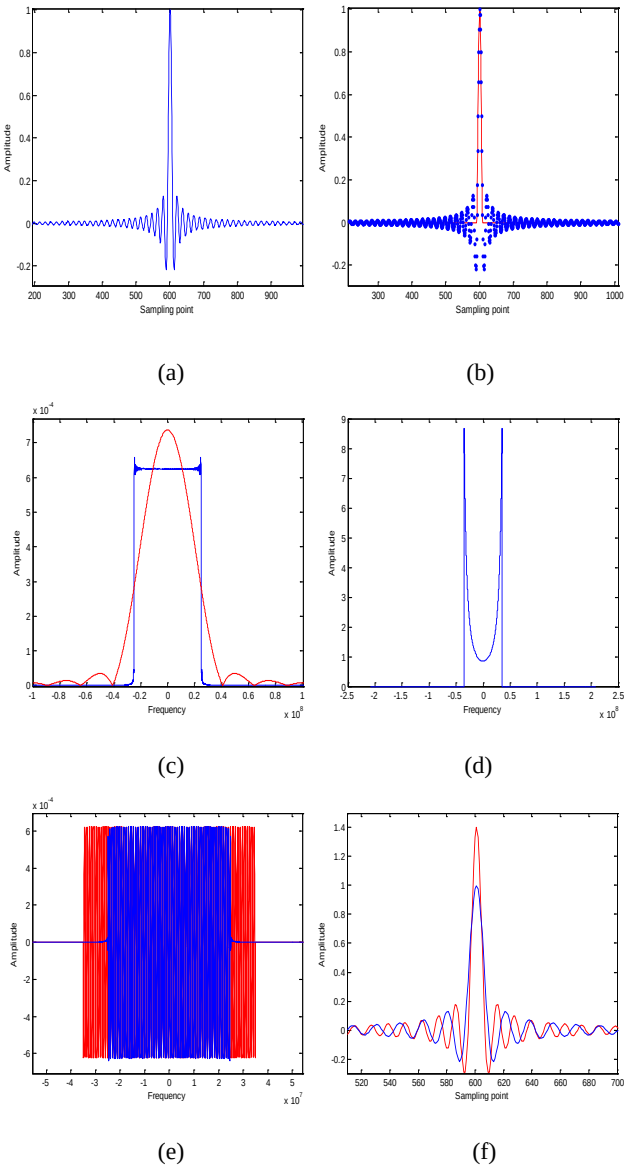

Fig.4: The signal processing flow chart of Super-SVA
(a) The echo signal from pulse compression
(b) The result after SVA
(c) The spectrum after SVA
(d) The inverse amplitude weighting operation
(e) The reshaped spectrum
(f) The result after Super-SVA

Super-SVA is a super-resolution method developed on the basis of SVA[11,12], the basic

process is described as follows. Firstly, the pulse compression is performed on the baseband signal of echo, and the result is shown in Figure 4 (a).Since SVA only saves the main lobe of the signal , the signal is equivalent to the time domain truncation by using SVA, shown as the red curves in Figure 4 (b). Thus, the frequency spectrum will be extrapolated, and the blue and red curves represent the frequency spectrum before and after SVA respectively shown as in Figure 4 (c). In order to improve resolution and save the information of target, the spread spectrum need be reshaped into a rectangle spectrum with the same amplitude, as shown in Figure 4 (e), where blue and red profile represent the frequency spectrum before and after extrapolation, respectively. Therefore, the spread spectrum need be multiplied by a frequency-domain inverse amplitude weighting operation, which is the amplitude ratio of extended rectangle spectrum and IFFT of a sinc function mainlobe, as shown in Figure 4 (d). Finally, after IFFT, the resolution of target is improved, as shown in Figure 4(f), where the blue and red curves represents the result before and after Super-SVA, respectively. The above extrapolation procedure can be repeated several times to get much higher resolution as desired.

4.2. Pseudo peak suppression by Super-SVA

In multi-carriers chirp, the introduction of the protection interval makes sub-band B less than the carrier frequency increment Δf, which results in the distance resolution of a pulse greater than the single point unambiguous range. So a single pulse contains more than one valid zone. Then, the valid zones are picked up from the fine distance dimension and are spliced in order. As a result, the false targets will arise in HRRP. Super-SVA is applied to extend bandwidth of sub-band, which makes pulse width smaller on coarse distance dimension. Here, the extended bandwidth notes as B'. As long as $B' > \Delta f$, a pulse width can be smaller than the single point unambiguous range. In this way, there is only one valid zone to be saved against one target in target extraction.

The flow chart of proposed algorithm is shown in Figure 5. Firstly, the channel division is performed on multi-carriers chirp echo, and the baseband echo signal in each channel passes through match filter. Afterward, IDFT is applied between different channels of the same sampling distance gate. To eliminate false targets generated by pseudo, Super-SVA is performed on each channel to decrease pulse width. After Super-SVA, the still existence of sidelobes can generate false targets and cover weak targets. Furthermore, RSVA[13] can be applied to suppress sidelobes under the noninteger Nyguist sampled version. By targets extraction, there is only one valid zone in a single pulse. Thus, the pseudo peaks are removed.

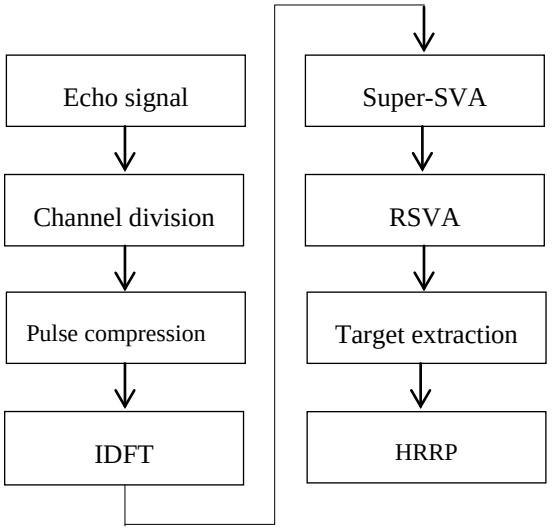

Fig.5: The flow chart of multi-carriers chirp processing

5. Simulation and analysis

5.1 Simulation for single target environment

Here are some simulation results. The parameters used in the simulation are listed in Table 1.

Table 1: Simulation parameters

Sub-chirp bandwidth (B)	50MHz
Pulse width (T)	2us
Initial carrier frequency (f_0)	2.4GHz
Increment of carrier frequency (Δf)	60MHz
Number of carriers (N)	20
Sampling resolution (R_s)	0.375m
Single point unambiguous range (R_I)	2.5m
Fine resolution (ΔR)	0.125m
Target distance (R)	15.125m

After pulse compression of baseband echo signal and RSVA, the result without Super-SVA is shown as Figure 6, where the center of pulse locates on $x_{mid} = 15m$, and both of the first zero point locate on $x_{left} = 11.63m$ and $x_{right} = 18m$. Since

$x_{mid} - x_{left} = 3.37 > R_I$, there is more than one sampling point, whose valid zone contains target, between x_{mid} and x_{left}. Similarly, it is the same between x_{mid} and x_{right}.

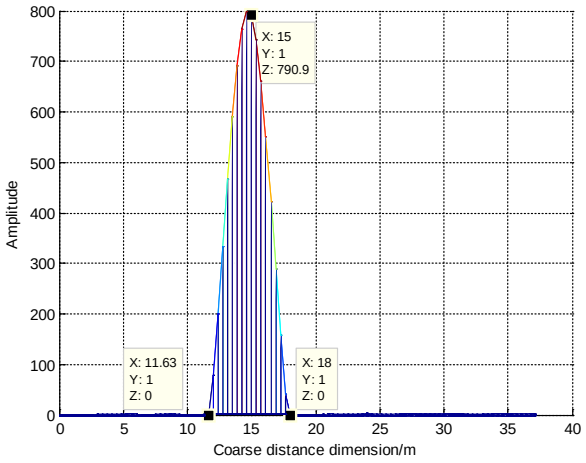

Fig.6: The amplitude diagram of coarse distance dimension without Super-SVA

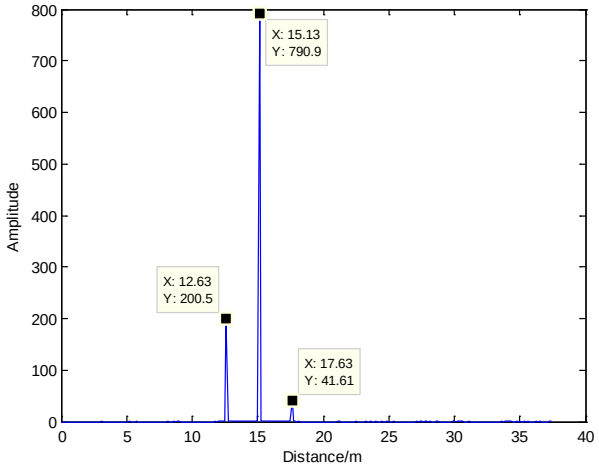

Fig.7: The HRRP without Super-SVA

Figure 7 shows the HRRP without Super-SVA, which had a false target on each side of target location $R = 15.13m$, respectively. And there is the distance of R_I from the real target to false targets.

In Figure 8, the blue profile represents the spectrum without Super-SVA after pulse compression, whose bandwidth is 50MHz, and the red profile represents one with Super-SVA, whose bandwidth is 80MHz. Obviously, the bandwidth is extended by 60% of the original signal.

The result with Super-SVA is shown as Figure 9, two first zero points locates on $x_{left} = 12.75m$ and $x_{right} = 16.88m$, so the width of target is $2.0650m$. In fact, the theoretical width of target should be $1.875m$ for $B = 80MHz$, the difference results from the error produced by sampling resolution. However, the width of target without Super-SVA is $c/2B = 3m$, this shows that the width of target is compressed and has been smaller than R_I. Therefore, only one valid zone can be picked up.

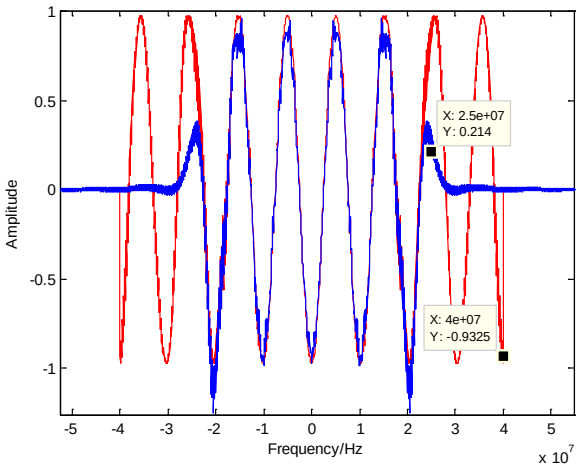

Fig.8: The Spread spectrum diagram with Super-SVA

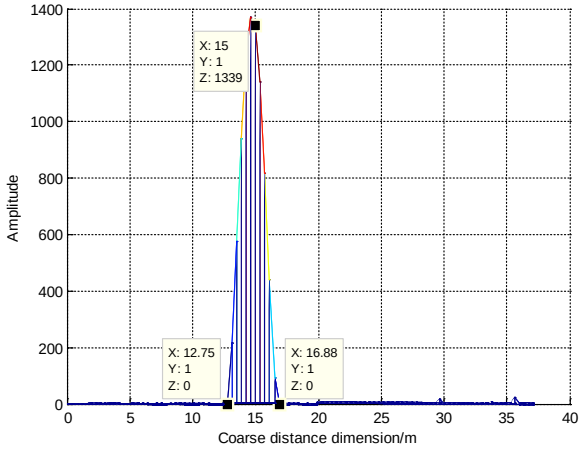

Fig.9: The amplitude diagram of coarse distance dimension with Super-SVA

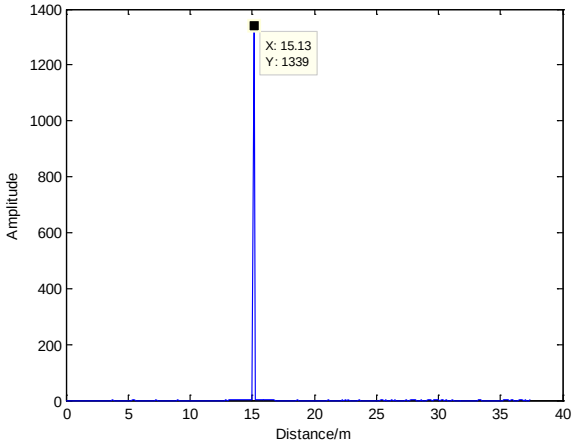

Fig.10: The HRRP with Super-SVA

It can be seen from Figure 10 that the false targets in both side of real target have disappeared. That means that the false targets generated by pseudo peaks can be removed effectively by using Super-SVA.

5.2 Simulation for multi-targets environment

We assume that three target distances are $R_1 = 19.250m$, $R_2 = 20.125m$, $R_3 = 20.750m$ and $RCS_1 = 1$, $RCS_2 = 0.6$, $RCS_3 = 0.3$, respectively. The other parameters are the same as table 1.

We can see from the simulation results that weak targets and false targets is difficult to be distinguished, in multi-target environment, as shown in Figure 11 (a) and.12 (a). Implementing Super-SVA on multi-carrier chirp, we can eliminate false target after RSVA and target extraction, as shown in Figure 11 (b) and Figure 12 (b).

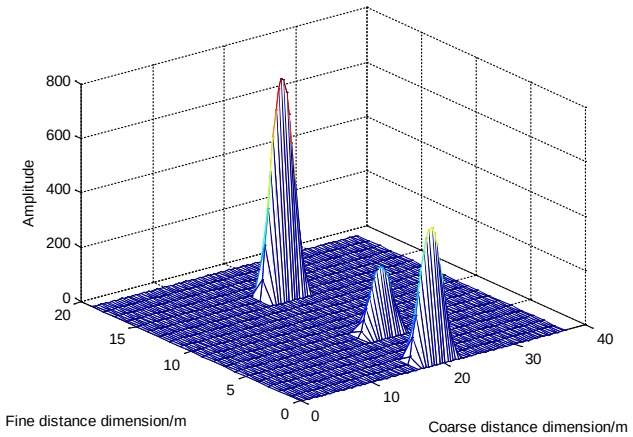

(a)

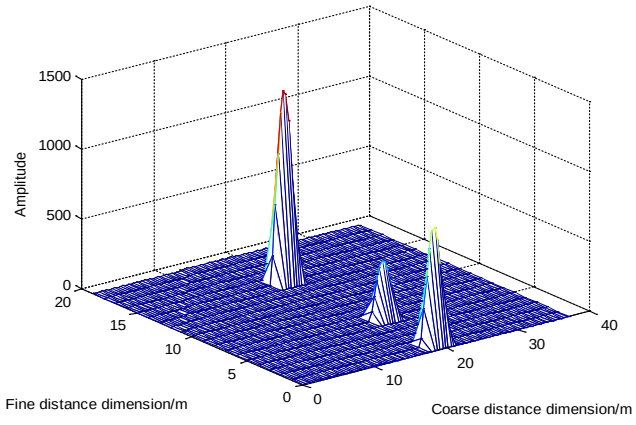

(b)

Fig.11: The 2 dimension range profile under $B < \Delta f$.
(a) The result without Super-SVA
(b) The result with Super-SVA

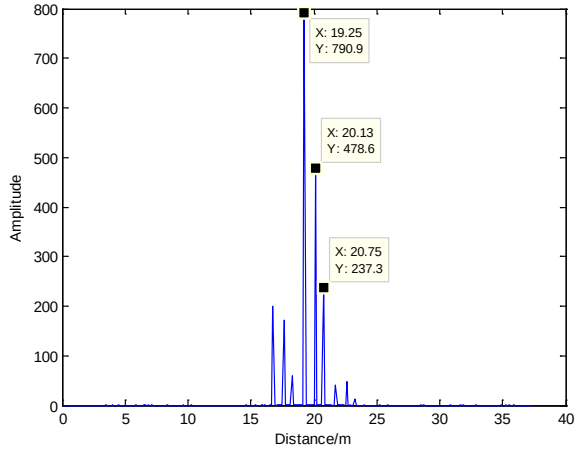

(a)

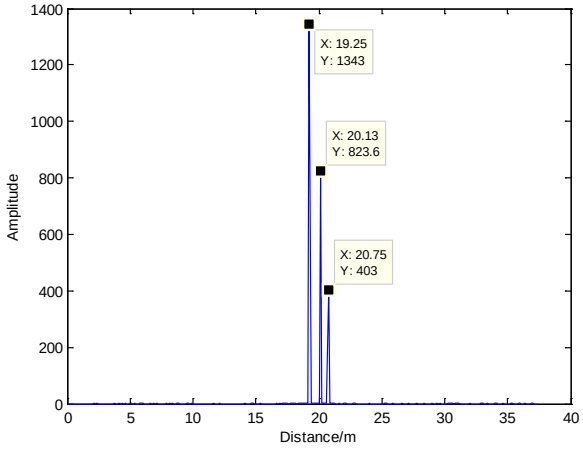

(b)

Fig.12:The HRRP without Super-SVA (a) and with Super-SVA (b)

6. Conclusion

This paper analyzes the causes of pseudo peaks generation on HRRP for multi-carrier chirp. Super-SVA is applied on multi-carrier chirp to decreases pulse width by bandwidth extrapolation. In target extraction, it can ensure that there is only one valid zone in the width of pulse in order to avoid the false peaks. Compared with the original process, the algorithm can avoid pseudo peaks and improve target resolution, just using Super-SVA algorithm before sidelobe suppression. With the simulation in single target and multiple targets environment, the results confirm the validity of the algorithm.

References:

[1] Zhang Ming-you. The Conspectus of Integrated Radar-EW-Communication. Beijing: National Defense Industry Press, 2010, pp. 87 - 101.

[2] Li Xiao-bo,Yang Rui-juan and Wei chen. Integrated Radar and Communication Based on

Multicarrier Frequency Modulation Chirp Signal. *Journal of electronics &information technology*, Vol.35, No.2, 2013, pp.406-412

[3] Yang Ming-lei, Zhang Shou-hong,Chen Bai-xiao and Zhang Huan-ying. A Novel Signal Processing Approach for the Multi-Carrier MIMO Radar. *Journal of electronics &information technology*, Vol.31, No.1, 2009, pp.147-151.

[4] Long Teng. Doppler Performance Analysis of Frequency Stepped Radar Signal, *Journal of modern radar*, Vol.18, No.2, 1996, pp.31-37 + 65.

[5] Xiong Zhang-liang, Shi Xiang-quan,Wang Zhi-hua and Zhao zhao. Analysis of Multicarrier Radar Signal, *Journal of modern radar*, Vol.29, No.10, 2007, pp.35-39.

[6] Long Teng,Li Dan and WU Qiong-zhi. Design Methods for Step Frequency Waveform and the Target Pick-up Algorithm. *Journal of systems engineering and electronics*, Vol.23, No.6, 2001 pp.26-31.

[7] Li Dan and Long Teng. Target's Redundance Removed Algorithms of Step Frequency Radar. *Journal of electronics*, Vol.28, No.6, 2000 pp. 60-63 + 67.

[8] Lei Wen,Long Teng and Han Yue-qiu.Novel Signal Processing Methods for Moving Targets in Stepped Frequency Modulated Radar. *Journal of electronics*, Vol.28, No.12, 2000, pp.34 -37.

[9] Zhang Huan-ying, Zhang Shou-hong and Li Qiang. Target Extracting Algorithm and System Parameter Design in Stepped Frequency Modulated Radar. *Journal of electronics*, Vol.35, No.6, 2007, pp.1153-1158.

[10] Long Teng,Mao Er-ke and He Pei-kun. Analysis and Processing of Modulated Frequency Stepped Radar Signal. *Journal of electronics*, Vol.26, No.12, 1998, pp.84-88.

[11] Zhang Huan-ying, Zhai W S. Apply super-SVA to stepped-frequency chirp signal processing based on dechirp method, 2nd *Asian-Pacific Conference on Synthetic Aperture Radar*. Xi'an: IEEE AESS and IEEE GRSS 2009,:431-434.

[12] NI Chong,WANG Yanfei, XU Xianghui,et al, A super-resolution algorithm for synthetic aperture radar based on modified spatially variant apodization. *Science China (Physics Mechasnics & Astronomy)*, Vol.54, No.2, 2011, pp.355-364.

[13] C. Castillo-Rubio, S. Llorente-Romano and M. Burgos-García, A new robust SVA method for every sampling rate condition, *IEEE Trans. ons on Aerospace and Electronic Systems*, Vol.43, No.2, 2007, pp.571-580

Acknowledgments

This work was supported by National Natural Science Foundation (project 61371107, project 61362006) of China, and Foundation of Key Lab. of Cognitive Radio & Information Processing, the Ministry of Education in China (project 2013ZR08), also supported by Science and Technology on Information Transmission and Dissemination in Communication Networks Lab. (Open project KX132600010 / ITD-U13003).